Int. J. Therm. Sci. (1999) 38, 113–120

Optimisation of film condensation with periodic wall cleaning

José Viriato Coelho Vargas, Adrian Bejan*

Department of Mechanical Engineering and Materials Science, Duke University, Durham, North Carolina, 27708-0300, USA

(Received 19 March 1998, accepted 20 July 1998)

Abstract—This is a theoretical and experimental study of the time-optimisation of condensation on a vertical wall when the film is removed periodically by a mechanical device. The objective is to fine-tune the periodic process so that the production of condensate and the heat transfer rate are maximal. The first part of the paper develops the scales of the periodic condensation process, and predicts the existence of an optimal condensation time interval. The analysis also predicts that the augmentation of condensation increases as the mechanical cleaning time decreases. These design optimisation opportunities are confirmed in the second part of the paper, which reports measurements of steam condensation on a vertical surface scraped periodically. (c) Elsevier, Paris. © Elsevier, Paris.

condensation / optima / rhythmic processes / thermodynamic optimisation

Résumé — Optimisation d'un film de condensat sur une paroi nettoyée périodiquement. On présente une étude théorique et expérimentale de l'optimisation du temps de condensation sur une paroi verticale, lorsque le film de condensat est enlevé périodiquement par un moyen mécanique. L'objectif est de caractériser le processus périodique au travers de la production de condensat et du flux de chaleur maximal. La première partie de ce travail définit l'échelle du processus périodique de condensation et prévoit l'existence d'un intervalle de temps optimal de condensation. L'analyse prévoit aussi que la quantité de condensat augmente avec la diminution du temps de nettoyage mécanique. Ce résultat théorique est confirmé dans la deuxième partie de ce travail, où on présente des résultats expérimentaux obtenus pour le cas de la condensation de vapeur d'eau sur une surface verticale nettoyée periodiquement. © Elsevier, Paris.

condensation / optimums / processus rythmiques / optimisation thermodynamique

Nomenclature

a	factor	$kg \cdot m^{-1} \cdot s^{-1/2}$
b	factor	$kg \cdot m^{-1} \cdot s^{-1}$
B	bias limit	
c_P	specific heat at constant pressure	$J \cdot kg^{-1} \cdot K^{-1}$
h_{fg}	latent heat of condensation	$J \cdot kg^{-1}$
h'_{fg}	augmented latent heat	$J \cdot kg^{-1}$
H	height	m
Ja	Jakob number	
k	thermal conductivity	$W \cdot m^{-1} \cdot K^{-1}$
m	mass	$kg \cdot m^{-1}$
$\dot{m}$	mass flow rate	$kg \cdot m^{-1} \cdot s^{-1}$
P	precision limit	
Pr	Prandtl number	
Pr_{film}	film Prandtl number	
r	dimensionless factor, equation (6)	
Ra_{film}	film Rayleigh number	
s	gap thickness	m
t	time	s
t	condensation time interval	s
t_c	cleaning time	s
t_f	total time of experimental run	s
U	uncertainty limit	
v	liquid film velocity	$m \cdot s^{-1}$
v_b	wiper velocity	$m \cdot s^{-1}$
$\dot{W}$	power	W
α	thermal diffusivity	$m^2 \cdot s^{-1}$
δ	film thickness	m
δ_b	wiper blade thickness	m
ΔT	temperature difference	K

* Correspondence and reprints.
abejan@acpub.duke.edu

ρ	liquid density	$kg \cdot m^{-3}$
ρ_v	vapor density	$kg \cdot m^{-3}$
τ	shear stress	$N \cdot m^{-2}$
$()_{max}$	maximum	
$()_{opt}$	optimum	

1. INTRODUCTION

It is well known that film condensation is inferior to drop condensation from the point of view of achieving high heat transfer and condensate production rates. In fact, the film condensation rate is roughly one order of magnitude smaller than the drop condensation rate on a wall of the same height and temperature. The reason for the great difference between the two condensation rates is also well known: in dropwise condensation, the movement of a large drop has the effect of cleaning a portion of the wall, getting it ready for an incipient condensation process that is ruled by time-dependent conduction and characterised by a high rate of condensation.

The idea investigated in this paper is to do artificially during film condensation what nature does in drop condensation. Specifically, we consider the *process* of periodic film condensation on a wall that is cleaned intermittently using, for example, a mechanical sweeper. Each cleaning stroke prepares the wall for a film condensation process in which the film grows starting from zero thickness, in a manner similar to the early stages of drop formation. We show that the periodic condensation and cleaning cycle can be optimised for a maximum time averaged rate of condensate production.

This study is part of a larger effort to identify fundamental optima [1] in the application of heat transfer phenomena that otherwise have been studied extensively (in isolation). Condensation is one process that has been studied extensively, and, consequently, to document its fine details is not the objective of the present work. To demonstrate the *existence* of an opportunity to optimise the process is the objective. This important difference between transport fundamentals and fundamental optima (the present objective) is further illustrated by the design of the experimental apparatus (section 4) and the thermodynamic considerations presented in section 5.

A survey of the condensation literature shows that although augmentation techniques have received considerable attention, the process optimisation opportunity described in this paper has not been investigated. For example, Dent [2] studied the effect of condenser tube vibration, and found a 15 percent increase in the condensation heat transfer coefficient. The same method was studied subsequently by Brodov et al. [3], who obtained a 20 percent increase in heat transfer coefficient. Uhl [4] reviewed the performance of several scraper agitators and close-clearance devices for single-phase heat transfer, and concluded that mechanical techniques are promising. Lustenader et al. [5] considered the conjugate configuration of film evaporation on the inner surface and film condensation on the outer surface, with mechanical wiping on the evaporation side.

2. BASIC SCALES OF TRANSIENT FILM CONDENSATION ON A VERTICAL WALL

The fundamentals of time-dependent film condensation have received considerable attention in the literature, beginning with the analyses of Sparrow and Siegel [6] for the wall with step change in temperature, and Cheng and Chui [7] for the saturated porous medium version of the same problem. The progress in this field was reviewed by Flik and Tien [8] who also developed a general analytical treatment for a broad class of condensation problems. Although compact analytical solutions are available [6], in this section we derive briefly the main scales of time-dependent film condensation: these scale-analysis results are accurate enough and their derivation will be relevant to the optimisation of the on-and-off process described in the next section.

Consider a vertical wall of height H in contact with a reservoir of quiescent vapour at saturation temperature T_{sat}. The wall is cooled to a lower temperature T_w, beginning at the time $t = 0$. By analogy with the time-dependent development of a vertical natural convection boundary layer in a single-phase fluid [9], immediately after $t = 0$ the heat transfer between the wall and the fluid is by pure conduction in the direction perpendicular to the wall. In the case of film condensation, the temperature difference $\Delta T = T_{sat} - T_w$ is bridged by a film of condensate of thickness δ and constant properties (k, ρ, c_p, ν, α, Pr). The heat transfer into the wall, $kH\Delta T/\delta$, is generated by condensation at the liquid-vapour interface that expands outward at the rate $d\delta/dt$:

$$k\,H\frac{\Delta T}{\delta} \sim \rho\, h_{fg}\, H\frac{d\delta}{dt} \tag{1}$$

Integrating this equation from $\delta(0) = 0$, we obtain $\delta(t) \sim (k\Delta T/\rho\, h_{fg})^{1/2}\, t^{1/2}$. The corresponding mass of condensate produced during the time t is:

$$m_1 \sim \left(\frac{\rho H^2\, k\, \Delta T}{h_{fg}}\right)^{1/2} t^{1/2} \tag{2}$$

This first regime is followed by the well known regime of steady film condensation (regime 2). In laminar flow with $Pr_{film} \gtrsim 1$, the scales of this second regime are [9]:

$$v \sim \frac{\alpha}{H}\, Ja\, Ra_{film}^{1/2} \tag{3}$$

$$\delta \sim H\, Ra_{film}^{-1/4} \tag{4}$$

where v is the vertical velocity of the liquid:

$$Ra_{\text{film}} = \frac{g\,(\rho - \rho_v) H^3 h'_{fg}}{\nu\, k\, \Delta T}, \quad Ja = \frac{c_P\, \Delta T}{h'_{fg}} \tag{5}$$

$$h'_{fg} = h_{fg} + (r) c_P \Delta T, \quad Pr_{\text{film}} = \frac{Pr}{Ja} \tag{6}$$

(r) is a numerical constant of order 1, and ρ_v is the vapour density.

The time scale that marks the transition from regime 1 to regime 2 is dictated by the time required by the liquid to sweep the wall height H:

$$t_{12} \sim \frac{H}{v} \sim \frac{H^2}{\alpha}\, Ja^{-1}\, Ra_{\text{film}}^{-1/2} \tag{7}$$

The condensate flow-rate in the second regime is $\rho v \delta$, and therefore the liquid mass generated from the start of this regime is $\rho v \delta (t - t_{12})$. In conclusion, the total mass of condensate produced beginning with $t = 0$ is:

$$m_2 = a\, t_{12}^{1/2} + b\,(t - t_{12}) \tag{8}$$

where (cf. equation (2)):

$$a = \left(\frac{\rho H^2\, k \Delta T}{h_{fg}} \right)^{1/2} \tag{9}$$

and

$$b = \frac{k}{c_P}\, Ja\, Ra_{\text{film}}^{1/4} \tag{10}$$

In summary, the condensate mass is given by equation (2) or $m_1 \sim a\, t^{1/2}$ when $t < t_{12}$, and by equation (8) when $t > t_{12}$. The complete time-dependent behaviour of the condensate mass $m(t)$ is illustrated in *figure 1*.

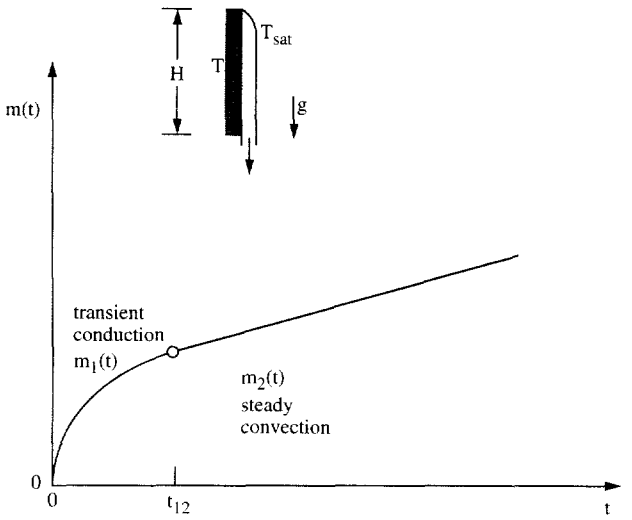

Figure 1. The time-dependent evolution of the mass of liquid generated on a vertical wall with film condensation.

3. PERIODIC WALL CLEANING

Figure 1 shows that the condensation rate dm/dt decreases with time, and reaches its lowest value during the second regime. In pursuit of a higher condensation rate, it makes sense to interrupt the film condensation process, clean the wall, and restart the process triggered at $t = 0$ in *figure 1*. The assumption that the film thickness becomes zero after each wiping stroke is an approximation, which depends on how finely the wiper can be adjusted and how large a friction loss can be tolerated (see section 5). The periodic process obtained in this manner is illustrated in *figure 2*. New in this figure is the time scale t_c, which is the cleaning time interval, or the time scale of the mechanical cleaning process. The condensation rate averaged over many condensation and cleaning cycles of period $(t + t_c)$ is:

$$\dot{m} = \frac{m(t)}{t + t_c} \tag{11}$$

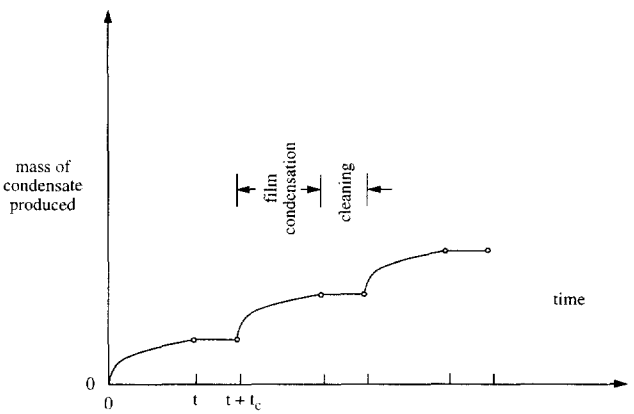

Figure 2. Cyclical process consisting of film condensation followed by wall cleaning.

where t is the duration of the film condensation portion of the cycle. The condensate collected during one cycle, $m(t)$, is given either by equation (2) or equation (8). The condensation rate $\dot{m}$ is a function of the condensation time t, which is a degree of freedom. The cleaning time t_c is assumed specified (constrained) by the design of the cleaning system. We distinguish the following possibilities according to the size of the condensation interval.

$\mathbf{t < t_{12}}$. Equation (11), in combination with equation (2), yields a function $\dot{m}(t)$ that has a maximum at:

$$t_{\text{opt}} \cong t_c\,, \qquad \dot{m}_{\max} \cong \frac{a}{2\, t_c^{1/2}} \tag{12}$$

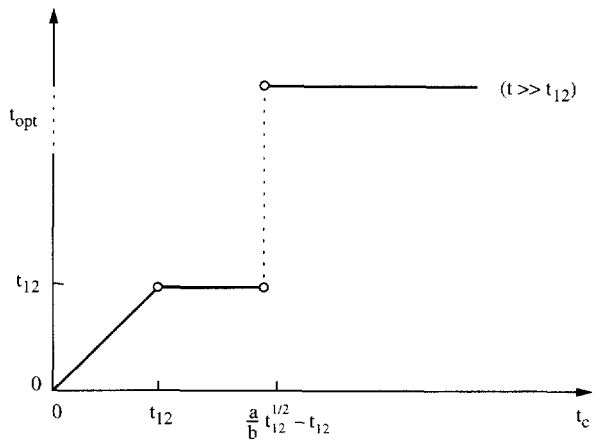

Figure 3. The optimal film condensation time interval.

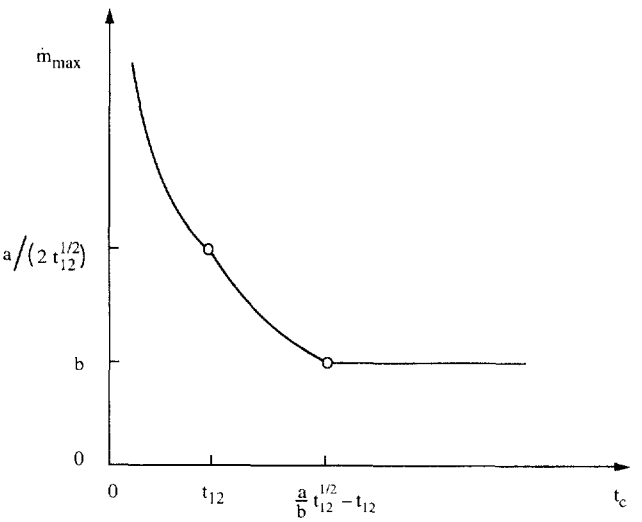

Figure 4. The maximum average condensation rate.

These results are shown in *figures 3* and *4*, and are valid when t_c is smaller than the transition time t_{12}. When t_c is greater than t_{12}, the largest $\dot{m}$ value (a supremum, not an extremum) is registered at:

$$t_* \cong t_{12}\,, \qquad \dot{m}_* \cong \frac{a\, t_{12}^{1/2}}{t_{12} + t_c} \tag{13}$$

$\mathbf{t > t_{12}}$. When the condensation interval is greater than the convection development time t_{12}, equation (11) combined with equation (8) yields a monotonic function $\dot{m}(t)$. Since the slope $d\dot{m}/dt$ is negative if

$$t_c < \frac{a}{b}\, t_{12}^{1/2} - t_{12} \tag{14}$$

the largest $\dot{m}$ value corresponds to the smallest t, namely the t_* and $\dot{m}_*$ values seen already in equation (13). This conclusion has been added to both *figures 3* and *4* on the assumption that $\left[(a/b)\, t_{12}^{1/2} - t_{12}\right] > t_{12}$.

If the reverse of the inequality (14) is true, then $\dot{m}$ increases monotonically approaching the plateau:

$$\dot{m}_{max} \cong b \tag{15}$$

This $t \gg t_{12}$ limit means that the largest average condensation rate is achieved when the film condensation part of the cycle operates in the steady state. When $\left[(a/b)\, t_{12}^{1/2} - t_{12}\right]$ is smaller than t_{12}, the middle segments disappear from the curves drawn in *figures 3* and *4*. It is worth noting that the quantity $(a/b)\, t_{12}^{1/2} - t_{12}$ is always positive: use equation (8) and *figure 1* to estimate the positive cut made by $m_2(t)$ on the ordinate $(t = 0)$.

To summarise the optimisation results plotted in *figures 3* and *4*, there corresponds to each cleaning interval t_c an optimal condensation interval t_{opt}. The maximised average condensation rate (*figure 4*) increases as the cleaning time decreases. This trend is particularly strong when t_c and, consequently, t_{opt} become shorter than the film convection development time t_{12}. The optimisation of the condensation and cleaning cycle is illustrated in the next section using an apparatus whose cleaning time was shorter than the film development time, $t_c < t_{12}$.

4. EXPERIMENTAL DEMONSTRATION

We constructed an apparatus (*figure 5*) and conducted a large number of measurements to demonstrate the existence of the optimal periodic condensation regime described in the preceding section. The objective of this experimental phase was to *optimise the design* of the condensation cycle, that is, to compare a large number of condensation regimes that varied only slightly with respect to cycle period. Our objective was not to document the details of the condensation process, because this aspect is amply documented in the heat transfer literature.

The apparatus was designed with the design-optimisation objective in mind. It combines accuracy and controllability on the cycle design side (*figure 5*, left) with simplicity and low cost in the condenser (*figure 5*, right).

Water was boiled at atmospheric pressure in a cylindrical vessel with a diameter of 180 mm, and a capacity of 3 300 cm^3. The vessel was insulated with fibreglass. It was heated from below by an annular heater at constant power (1 200 W at 120 V and nominal resistance 12 Ω). The vessel was placed under the supporting table shown in *figure 5*. An insulated

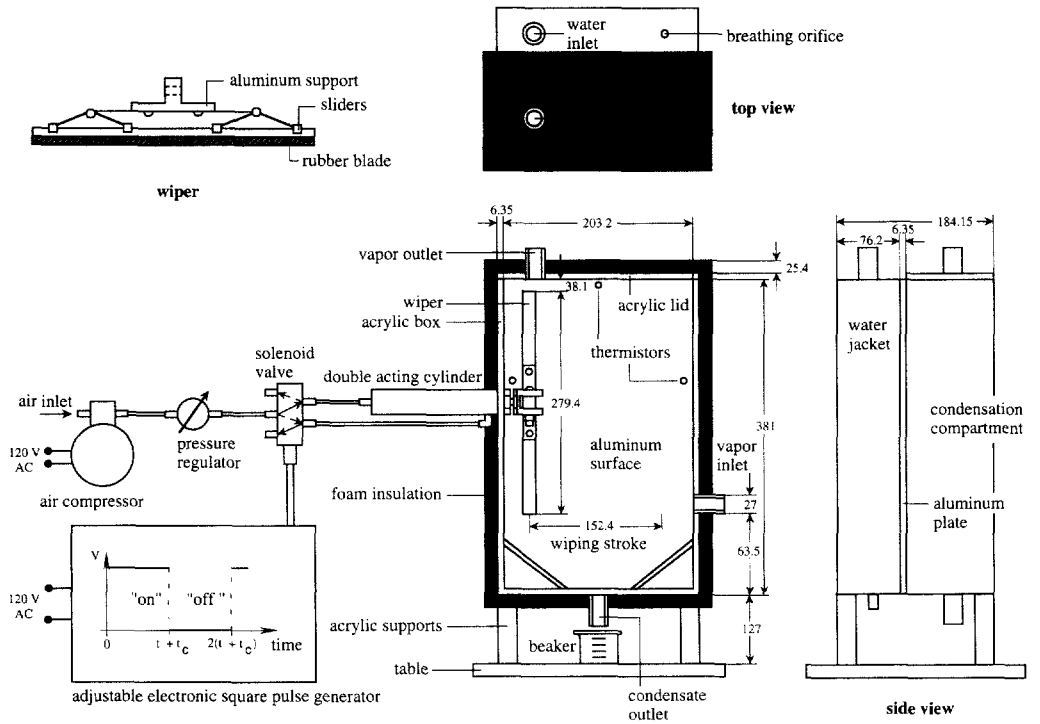

Figure 5. The main features and dimensions of the experimental apparatus.

hose collected the steam from the vessel and led it into the condensation compartment of the apparatus. That compartment was insulated with foam and fitted with an acrylic lid with vent port. The condensed water was collected from the bottom of the compartment into a graded beaker.

The condensing surface was a 0.4 m-tall and 0.64 cm-thick aluminium plate cooled from behind by a heat exchanger supplied with tap water. The aluminium surface was cleaned intermittently by a rubber wiper, which was driven by a pneumatic double action cylinder. The air was supplied by a compressor. The motion inside the double action cylinder was controlled by a solenoid directional valve. As shown in the lower-left corner of *figure 5*, the valve was driven by a step function with constant voltage from $t = 0$ to $t + t_c$, and zero voltage during the next interval of the same length. This resulted in a wiping stroke, either to the right or to the left, in which the cleaning time (t_c) is the time of travel across the aluminium surface. We varied the cleaning time by using a pressure regulator to vary the driving pressure in the pneumatic circuit.

We designed and built the adjustable electronics needed to assemble our own square wave to control the condensation (waiting) time t. The time interval $(t + t_c)$ was controlled by a dual timer integrated circuit of a standard type (No. 556), which controlled a relay that interrupted the power supply. The condensation time t could be adjusted. All the time interval settings were adjusted using a chronometer with a bias limit of ± 0.01 s.

Three high precision thermistors of type YSI 44004 (resistance 2 250 Ω at 25 °C) were embedded to a depth of 1 mm into the condensation side of the aluminium surface. Each thermistor had a standard Bead I with a 2.4 mm diameter. A layer of heat sink silicone was placed between thermistors and aluminium. *Figure 5* shows the thermistor locations on the aluminium surface. A fourth thermistor was suspended in the middle of the condensation compartment. Steady-state temperature readings were achieved between 50 or 60 s after the start of each run. The surface temperature readings were approximately 50 °C with a variation within 3 °C, which represents 7.5 percent of the temperature difference between the steam and the aluminium surface. The fourth thermistor measured a steam temperature of 90 °C with variations of less than 1 °C, indicating the presence of air in the condensation compartment.

The thermistor readings were taken with an ohmmeter capable of measuring resistances as small as 10^{-3} Ω in the temperature range of our experiments. We performed our own thermistor calibration to determine the bias limits. The thermistor was immersed in a constant temperature bath maintained by a bath circulator, and a total of 64 temperature measurements were made at 20, 30, ..., 120 °C. The largest standard deviation of

these measurements was 0.0005 °C, and therefore the bias limit was set at ± 0.001 °C for all thermistors. This bias limit is in agreement with the ± 0.0003 °C bias limit of the same thermistors in a natural convection experiment [10] and with the ± 0.0005 °C bias limit listed in an instrumentation handbook [11].

The experimental runs were performed while the transparent acrylic enclosure was insulated with foam. In order to observe visually the formation of the condensate film and its removal, we performed several preliminary runs without the insulation. The continuous film was very clear, especially when the interval between two sweeps was relatively long. For the measurements reported in this section, the total mass of condensate collected at the end of each run was:

$$m_f = \rho_l V_f \tag{16}$$

where V_f is the volume of condensate collected in the beaker of *figure 5*. This volume was measured later in the graded cylinder (bias limit ± 0.1 mL).

The electronic time control method rendered the precision limits negligible relative to the bias limit in the measurement of t and t_c. Five runs were executed for each of the points plotted in *figures 6* and *7*. The time t_f is the total (final) time of each run. The precision limit of the V_f measurements was taken as twice the standard deviation of each set of five V_f values. The number of runs per point was limited to five because of the violence of the wiping stroke, and the need to keep the apparatus adjusted and leak-proof during all the runs performed at a certain cleaning time t_c and final time t_f. In the computation of the uncertainty for m_f, the precision and bias limits of density were found negligible with respect to the volume measurements precision and bias limits. The uncertainty limits for m_f, t, t_c and T were calculated with the following formulas:

$$U_{m_f} = \rho_l (P_{V_f}^2 + B_{V_f}^2)^{1/2} \tag{17}$$

$$U_t = B_t \tag{18}$$

$$U_{t_c} = B_{t_c} \tag{19}$$

$$U_T = (P_T^2 + B_T^2)^{1/2} \tag{20}$$

These values are reported in *table I*. In addition, U_t and U_{t_c} were equal to 0.01 s in all the measurements.

A noteworthy feature of the apparatus construction was the use of a cleaning time t_c shorter than the film development time t_{12}, so that the optimisation of the condensation time t would be possible, cf. *figures 3* and *4* and the discussion under equation (15). For example, by using the experimental conditions (ΔT = 40 °C, H = 0.4 m) in equation (7), we find that t_{12} = 0.96 s, which is larger than the cleaning times used in the experiments. Indeed, *figure 6* shows that the production of condensate reaches a peak at a certain condensation time t_{opt}. This optimal time is comparable (in an order of magnitude sense) with t_c.

The cleaning time (t_c) and the total run time (t_f) were fixed for each of the runs summarised in *figure 6*.

TABLE I
The measured condensation cycle interval (t), cleaning time (t_c), total run time (t_f), and final mass of condensate (m_f), and the respective uncertainties.

	t_c=0.1 s			t_c=0.3 s
t_f(min)	3	6	10	6
t(s)	m_f(g) U_{m_f}(g)	m_f(g) U_{m_f}(g)	m_f(g) U_{m_f}(g)	m_f(g) U_{m_f}(g)
0.4	–	60.5 1.8	124.3 2.2	57.2 1.2
0.5	16.7 0.5	–	–	–
0.7	18.2 1.1	–	–	58.4 1.0
1.0	19.6 0.6	66.2 1.6	–	–
1.2	–	–	–	60.7 1.3
1.3	–	67.3 1.1	–	–
1.4	–	–	130.5 3.2	–
1.6	19.9 1.1	–	–	–
1.9	19.0 1.4	66.1 2.4	128.2 2.6	59.2 1.6
3.3	16.3 1.4	–	–	–
5.0	14.1 1.5	53.2 1.9	108.8 1.8	50.1 1.9
7.0	12.0 1.8	48.9 2.6	104.1 2.4	–
12.1	–	–	100.0 2.6	–
12.2	–	46.3 1.4	–	42.7 1.7
12.7	10.6 2.0	–	–	–
steady	7.6 0.5	38.1 2.0	92.3 1.4	38.1 2.0

The condensation time interval (t) was varied in the search for the maximum in the amount of condensate (m_f) collected at the end of each run. The horizontal line (asymptote) plotted on the right side of each frame corresponds to the limit $t \to \infty$, i.e., runs in which the wiper was not activated. The m_f maximum is clear; however, its relative amplitude varies with both t_f and t_c. The first three frames (*figures 6a-c*) show that the maximum is relatively sharper when the experiments are run for times t_f shorter than approximately 10 min. This trend is due to the fact that the condensation compartment needs about 10 min to approach its steady state, by wetting its bottom surfaces and purging most of the air. We investigated the approach to steady state in the experiments reported in *figure 7*, which were run in the absence of wiper motion. In *figures 6a-c* we used t_f values comparable with the time constant of the apparatus (10 min) because of an important construction limitation: the vibrations caused by each wiper stroke had to be kept to a minimum, because of potential misalignments in wiper motion, leaks, etc. This pushed the experimental demonstration toward the smallest and still meaningful t_f values.

The $\dot{m}$ values reported in *figure 7* were calculated from $\dot{m} = m_f/t_f$. The corresponding uncertainty limits were calculated with the formula $U_{\dot{m}}/\dot{m} = U_{m_f}/m_f$, and are reported in *table II*. The t_f uncertainty is negligible relative to the m_f uncertainty. A comparison with Nusselt's theory for steady state film condensation is

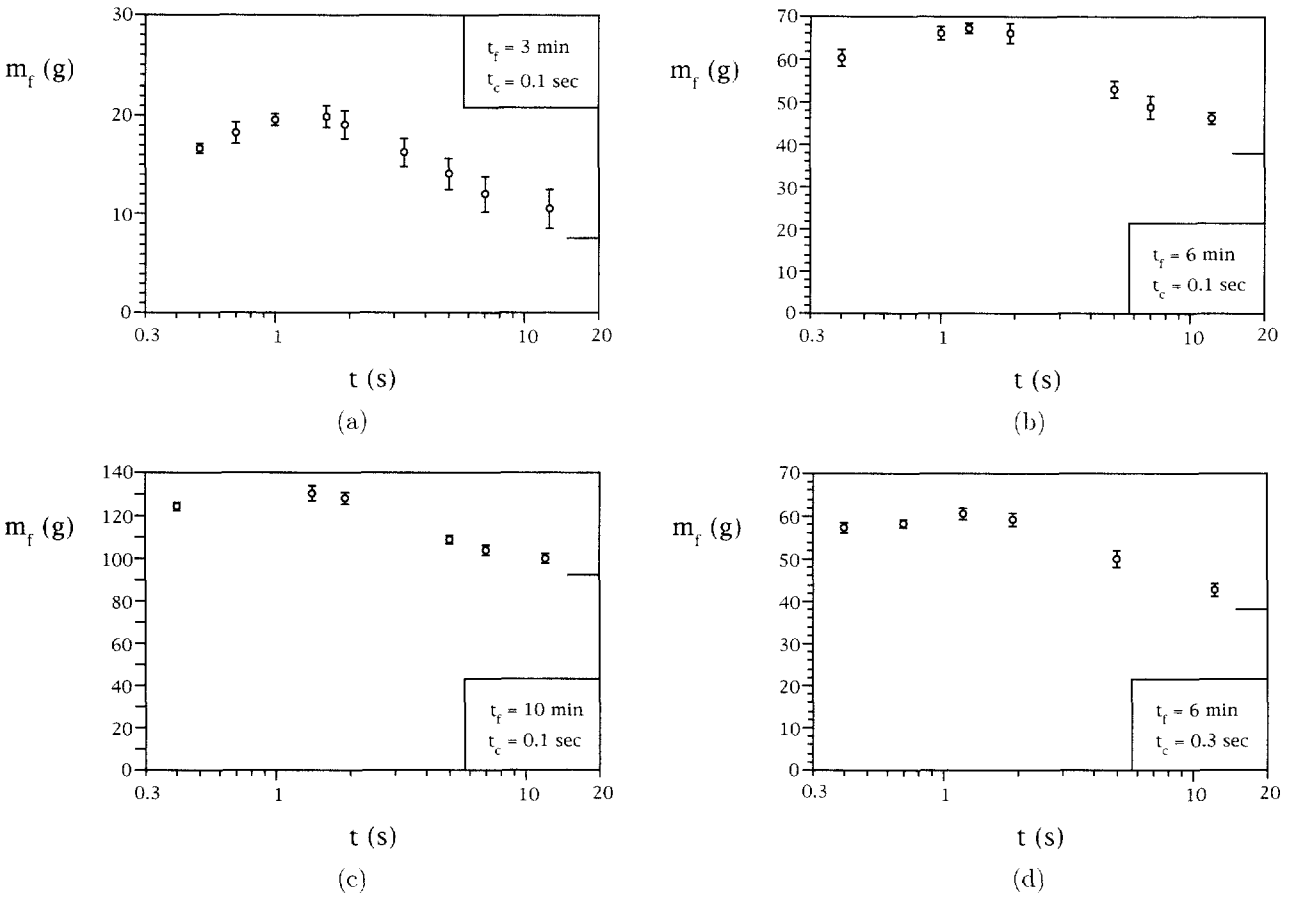

Figure 6. Measurements showing the maximisation of condensate production by varying the condensation time interval t.

TABLE II
The measurements and uncertainties associated with the experiments reported in figure 7.

t_f	m_f(g)	U_{m_f}(g)	$\dot{m}$	$U_m/\dot{m}$
3	7.6	0.5	2.5	0.066
6	38.1	2.0	6.4	0.052
10	92.3	1.4	9.2	0.015
12	117.8	6.8	9.8	0.058
14	141.2	6.7	10.1	0.048
17	173.5	9.9	10.2	0.057
20	209.4	13.3	10.5	0.064

not made, because in our experiments non-condensable gases (air) were present in the gaseous mixture. It is well known that the heat transfer coefficient and condensation rate are lower when non-condensable gases are present.

Figure 6d can be compared directly with *figure 6b* to see the effect of changing the cleaning time t_c. The relative condensation augmentation effect increases as the cleaning time becomes shorter. This trend confirms the expectations based on scale analysis, which were summarised at the end of section 3.

5. THERMODYNAMIC CONSIDERATIONS

In this paper we used scale analysis and direct measurements to demonstrate the existence of an optimal time regime of periodic cleaning during film condensation on a vertical wall. The quest for the highest average condensation rate (and highest heat transfer rate) pushes the design toward the shortest cleaning time possible. This trend runs eventually into mechanical difficulties: the sweeper must run at progressively higher speeds and frictional power loss. The smallest practical t_c emerges as a trade-off between

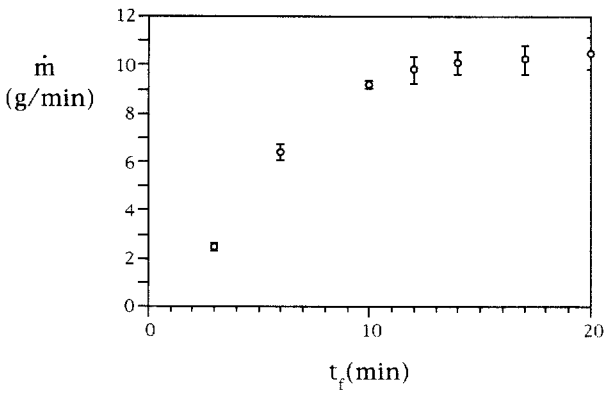

Figure 7. The effect of the duration of the experiment on the time-averaged condensation rate in the absence of wiper motion.

a higher condensation rate and a less reliable, or less efficient, sweeping device.

This trade-off can be illustrated analytically by comparing the competing effects on the same basis. The power destroyed by friction between the sweeper and the wall is $\tau \delta_b v_b$, where τ is the frictional shear stress, δ_b is the wiper blade thickness, and v_b is the wiper speed. If the sweeper slides on a very thin layer of condensate of thickness s, then $\tau \sim \mu v_b/s$, and the power loss is proportional to v_b^2 or t_c^{-2}.

The power destroyed by the irreversibility of heat transfer through the film is $q(\Delta T)/T_w$, where the total heat transfer rate q is proportional to the condensation rate $\dot{m}_{max} \cong a/2t_c^{1/2}$, in which $a = (\rho H^2 k \Delta T/h_{fg})^{1/2}$. In a heat transfer augmentation application such as the condensation optimisation performed in this article, the practical objective is to minimise ΔT when the heat transfer rate is specified (Bejan [12], p. 99). This means that the power lost due to heat transfer irreversibility $q\Delta T/T_w$ varies as ΔT, and, in turn, ΔT varies as $t_c^{1/2}$ because $\dot{m}$ (or q) is specified.

In summary, the time-averaged mechanical power destroyed by sweeper friction and film heat transfer across a finite ΔT is:

$$\dot{W}_{lost} = \underbrace{c_1 t_c^{-2}}_{\text{friction}} + \underbrace{c_2 t_c^{1/2}}_{\text{heat transfer}} \qquad (21)$$

where c_1 and c_2 are shorthand for the constant factors described in the preceding two paragraphs. The power loss is large when either effect dominates ($t_c \to 0$ or $t_c \to \infty$). It reaches a minimum value when the two effects are relatively in balance, namely at $t_{c,opt} = (4c_1/c_2)^{2/5}$ when the ratio (friction)/(heat transfer) in equation (21) is exactly 1/4.

The rhythmic process optimised in this paper is conceptually analogous to the pulsating processes that occur in living systems, for example, breathing and heart beating. This analogy is a most fascinating contribution of thermodynamic optimisation to the theory of organisation in natural systems, animate and inanimate. The reader is directed to reference [1] for a review of the current progress in this direction.

Acknowledgement

This work was supported by the National Science Foundation.

REFERENCES

[1] Bejan A., Advanced engineering thermodynamics, second ed., John Wiley and Sons, New York, 1997.

[2] Dent J.C., Effect of vibration on condensation heat transfer to a horizontal tube, Proc. Instn. Mech. Eng. 184 (1969-1970) 99–105.

[3] Brodov Y. M., Salev'yev R.Z., Permayakov V.A., Kuptsov V.K., Gal'perin A.G., The effect of vibration on heat transfer and flow of condensing steam on a single tube, Heat Transfer Soviet Res. 9 (1977) 153–155.

[4] Uhl V.W., Mechanically aided heat transfer to viscous materials, Augmentation of Convective Heat and Mass Transfer, ASME, New York, 1970.

[5] Lustenader E.L., Richter R., Neugebauer F.J., The use of thin films for increasing evaporation and condensation rates in process equipment, J. Heat Trans.–T. ASME 81 (1959) 297–307.

[6] Sparrow E.M., Siegel R., Transient film condensation, J. Appl. Mech. 26 (1959) 120–121.

[7] Cheng P., Chui D.K., Transient film condensation on a vertical surface in a porous medium, Int. J. Heat Mass Tran. 27 (1984) 795–798.

[8] Flik M.I. and Tien C.L., An approximate analysis for general film condensation transients, J. Heat Trans.–T. ASME 111 (1989) 511–517.

[9] Bejan A., Convection heat transfer, 2nd ed., John Wiley and Sons, New York, 1984, pp. 146–151, 159–164.

[10] Howle L., Georgiadis J., Behringer R., Shadowgraphic visualization of natural convection in rectangular-grid porous layers, ASME HTD 206-1 (1992) 17–24.

[11] Dally J.W., Riley W., McConnell K.G., Instrumentation for engineering measurements, John Wiley and Sons, New York, 1993.

[12] Bejan A., Entropy generation through heat and fluid flow, John Wiley and Sons, New York, 1982.